Guided ion beam studies of the reaction of Ni_n^+ ($n=2-16$) with D_2: Nickel cluster-deuteride bond energies

Fuyi Liu, Rohana Liyanage, and P. B. Armentrout
Department of Chemistry, University of Utah, Salt Lake City, Utah 84112

(Received 15 February 2002; accepted 8 April 2002)

The kinetic-energy dependences of the reactions of Ni_n^+ ($n=2-16$) with D_2 are studied in a guided ion beam tandem mass spectrometer. The products observed are Ni_nD^+ for all clusters and $Ni_nD_2^+$ for $n=5-16$. Reactions for formation of Ni_nD^+ are observed to exhibit thresholds, whereas cross sections for formation of $Ni_nD_2^+$ ($n=5-16$) exhibit no obvious barriers to reaction. Rate constants of D_2 chemisorption on the cationic clusters are compared with results from previous work on neutral nickel clusters. Ni_n^+-D bond energies as a function of cluster size are derived from threshold analysis of the kinetic-energy dependence of the endothermic reactions, and are compared to previously determined metal–metal bond energies, $D_0(Ni_n^+-Ni)$. The bond energies of Ni_n^+-D generally increase as the cluster size increases, and parallel those for Ni_n^+-Ni for many clusters. These trends are explained in terms of electronic and geometric structures for the Ni_n^+ clusters. The bond energies of Ni_n^+-D for larger clusters ($n\geqslant 11$) are found to be close to the value for chemsorption of atomic hydrogen on bulk phase nickel. © *2002 American Institute of Physics.* [DOI: 10.1063/1.1481855]

I. INTRODUCTION

Investigating the chemical reactivity, catalytic properties, magnetic properties, electronic structure, and geometries of small metal and transition metal clusters is currently an active frontier in chemical physics. One of the motivations for these studies is to determine the relation between reactivity and geometric and electronic structure. Studies of the reactivity of metal clusters of different charges and sizes have found that the reactivity can vary appreciably at small sizes, but that the size effects gradually vanish with increasing size.[1–10] From a fundamental point of view, such studies of cluster reactions are important because they offer opportunities to bridge the gap between gas and condensed phase chemistry. In addition, such studies may provide quantitative data concerning the elementary steps that make up complicated surface reactions, and thus help us to understand surface science at the molecular level. In elucidating the geometrical and electronic structures of clusters, spectroscopic techniques generally fail for larger clusters; hence, such information has been sought using chemical probes.

In the past two decades, the reactions of neutral nickel clusters with hydrogen and deuterium have been investigated extensively.[11–28] On the experimental side, Smalley and co-workers[11] measured the relative reaction rate constants for D_2 dissociation on various size neutral nickel clusters, Ni_n ($n=3-20$). The authors found that D_2 chemisorbs readily on nickel clusters and that the reaction rates increase slowly and in a nearly monotonic way as a function of cluster size. Riley and co-workers[12] observed a similar reactivity dependence on size, but with the important exception that the nine-atom cluster was an order of magnitude less reactive than other clusters. The rate constants were found to scale roughly with $n^{2/3}$ in the size range $n=4-13$, indicating a surface area dependence consistent with a hard-sphere model. Riley and co-workers have also examined the reaction of nickel clusters with deuterium over the temperature range 133–413 K.[13] For $Ni_{10}-Ni_{14}$, the reaction probabilities are near unity and essentially independent of temperature. For Ni_9, the reaction probability is about 5% between 213–413 K, but increases below 213 K to about 50% at 133 K. This increase is attributed to initial trapping of the D_2 molecule on the cluster surface. In addition to kinetics studies, these authors also measured the composition of nickel clusters saturated with H_2 and D_2.[14–16] They have found that the number of chemisorbed H or D atoms is also proportional to $n^{2/3}$. Recently, Riley and co-workers[17] also studied reactions of Ni_{19} and Ni_{23} with hydrogen/deuterium and ammonia to probe adsorbate-induced cluster structural changes.

Theoretical studies[18–28] of the dissociative absorption of D_2/H_2 on small nickel neutral clusters have been carried out by three groups. Jellinek and co-workers[18,19] have carried out molecular dynamics simulation studies of D_2 interacting with Ni_{13} having various geometrical structures. Here, the dependence of the reaction rate on both the internal energy of the cluster as well as on the initial rovibrational excitation of D_2 has been determined. They also calculated the structures and energies of nickel clusters ($n=7-14,19$) and cross sections and rate constants for reaction with the ground-state D_2 molecule.[20,21] DePristo and co-workers[22–24] have performed dynamics calculations for the reaction of the D_2 molecule in its ground rovibrational state with rigid and nonrigid nickel clusters in the size range $n=4-13$. It was found that the reaction rate constants vary strongly with size for clusters smaller than Ni_9 and vary over two orders of magnitude, depending on the assumed cluster structure for all cluster sizes. However, their calculated rates are much smaller than the experimental values.[12,13] Jellinek and Güvenç[19] postulate that this is a weak Ni–D interaction potential [about 10%

 © 2002 American Institute of Physics

lower than the measured energy of binding of a D atom to the (111) and (100) surfaces of bulk nickel[29]] was used in the dynamics calculation. Doll, Freeman, and co-workers[25–27] have calculated the geometries, the preferred binding sites, site-specific hydrogen normal mode frequencies, and finite temperature effects of mono- and di-hydrogenated nickel clusters using both classical and quantum mechanical Monte Carlo methods. In addition, the effects of hydrogen–hydrogen interactions on selected structural and time-dependent properties of hydrogen containing nickel clusters have been examined.

Our group has studied the collision-induced dissociation of the cluster ions of several transition metals[30–39] and their reactions with O_2,[40–42] CO_2,[43,44] D_2,[45–47] and CD_4[48] in an ongoing effort to understand the reactivity, electronic structure, and geometry of transition metal clusters. These experimental studies have shown interesting variations with cluster size in the stability and reactivity of clusters. In the present study, we use guided ion beam tandem mass spectrometry to investigate the reactions of size-selected nickel cluster cations Ni_n^+ ($n=2-16$) with D_2. Kinetic-energy dependent cross sections for formation of $Ni_nD^+ + D$ and $Ni_nD_2^+$ product channels are determined. The former are interpreted to provide Ni_n^+-D BDEs as a function of cluster size. Bond energy information for the larger clusters obtained here is favorably compared to bulk phase values. Rates of D_2 chemisorption on the cationic clusters are compared with results from previous work on neutral nickel clusters.

II. EXPERIMENT

Reactions of nickel cluster cations with D_2 are studied using a guided ion beam apparatus equipped with a laser ablation cluster source. The experimental apparatus and techniques have been described in detail elsewhere,[49] and only a brief description is given here. Nickel cluster cations are formed in a laser vaporization source.[50,51] The output (511 and 578 nm) of an Oxford ACL 35 copper vapor laser operating at 7 kHz is tightly focused onto a continuously translating and rotating nickel rod inside an aluminum source block. The optimum pulse energy for nickel cluster ion production ranges between 3–4 mJ/pulse. The vaporized material is entrained in a continuous flow ($5-6\times10^3$ sccm) of He passing over the ablation surface. Frequent collisions and rapid mixing lead to the formation of thermalized clusters as they travel down a 2 mm diameter$\times$63 mm long condensation tube. Although direct measurements of the internal temperatures of the clusters are not possible, previous studies have indicated that the clusters are not internally excited and likely to be near room temperature.[36,49]

This seeded helium flow then undergoes a mild supersonic expansion in a field free region that is skimmed, and passes through two differentially pumped regions. Positively charged ions are accelerated and injected into a 60° magnetic sector momentum analyzer. The mass-selected ions are decelerated and focused into a rf octopole ion guide[52,53] that extends through a reaction cell. The octopole beam guide is biased with dc and rf voltages. The former allows accurate control of the translational energy of the incoming ions, whereas the latter establishes a radial potential that efficiently traps the parent and product ions that travel through the octopole. The pressure of D_2 neutral reactant gas (99.8% purity) in the reaction cell is kept relatively low to reduce the probability of multiple collisions with the ions. To test this, all studies were conducted at two pressures of D_2, ~0.2 and ~0.4 mTorr. The resultant cross sections exhibited no pressure dependence for all cluster sizes, verifying that the results presented here result exclusively from single ion-molecule collisions. The product and reactant ions drift to the end of the octopole, where they are extracted, and injected into a quadrupole mass filter for mass analysis. Ion intensities are measured with a Daly detector[54] coupled with standard pulse counting techniques. Reactant ion intensities ranged from $2-8\times10^5$ ions/s. Observed product intensities are converted to absolute reaction cross sections as discussed in detail elsewhere.[53] Absolute errors in the cross sections are on the order of $\pm30\%$.

Results for each reaction system were repeated several times to ensure their reproducibility. CID experiments with Xe were performed on all cluster ions to ensure their identity and the absence of any excessive internal excitation. In all instances, CID thresholds are consistent with those previously reported.[36] The absolute zero in the kinetic energy of the ions and their energy distributions (0.7–2.0 eV, gradually increasing with cluster size) were measured using the octopole as a retarding energy analyzer.[53] The error associated with the zero of the absolute energy scale is 0.05 eV in the lab frame. Kinetic energies in the laboratory frame are converted to center-of-mass (CM) energies using the stationary target approximation, $E(\mathrm{CM})=E(\mathrm{lab})\ m/(m+M)$ where m and M are the masses of the neutral and ionic reactants, respectively. The data at the lowest energies are corrected for truncation of the ion-beam energy distribution.[53]

Products observed in this work include Ni_nD^+ and $Ni_nD_2^+$ species. Accurate measurements of the intensities of these species depend on our ability to resolve and transport them efficiently to the detector. Resolving the high intensity Ni_n^+ reactant ions from the low intensity Ni_nD^+ product ions proved to be difficult even when the quadrupole mass analyzer was set to operate at high resolution. In principle, the resolution could be increased sufficiently to separate the parent and product ions, but as this limit is approached, the transmission of the ions is reduced to the extent that the experiments become impractical and inaccurate. Therefore the experiments are conducted using D_2 (to maximize the resolution) and by adjusting the resolution of the quadrupole mass filter to be as high as possible without reducing the product ion intensities. Product intensities are accurately determined by measuring the ion intensities 2 and 4 amu above the reactant ion mass with and without D_2 gas in the reactant cell. The difference between these foreground and background measurements yields the intensity of the Ni_nD^+ and $Ni_nD_2^+$ products. Under the resolution conditions used, the peak for the $Ni_nD_2^+$ product overlaps that for the Ni_nD^+ product, however, these two products do not appear over the same kinetic-energy ranges, as verified by studies at higher mass resolution. We verified that changes in the mass resolution did not affect the kinetic-energy dependence of these

cross sections and hence the threshold analyses.

III. THRESHOLD ANALYSIS AND THERMOCHEMISTRY

The energy dependences of cross sections for endothermic processes in the threshold region can be modeled using Eq. (1),[55–57]

$$\sigma(E) = \sigma_0 \sum g_i (E + E_i - E_0)^N / E, \quad (1)$$

where σ_0 is an energy independent scaling parameter, N is an adjustable parameter, E is the relative kinetic energy, and E_0 is the threshold for reaction at 0 K. The summation is over the rovibrational states of the clusters having energies E_i and populations g_i, where $\Sigma g_i = 1$. Vibrational frequencies for the bare metal clusters are obtained by using an elastic cluster model suggested by Shvartsburg *et al.*[58] In this study, the parameters used are the Debye frequency for bulk nickel, $\nu_D(\infty) = 268\ \mathrm{cm}^{-1}$,[59] the bulk maximum longitudinal frequency, $\nu_{L,\max} = 296\ \mathrm{cm}^{-1}$,[59] and the ratio of the longitudinal to the transverse phonon velocity, $c_L/c_T = 1.79$.[60] The model cross section, Eq. (1), is also convoluted with the kinetic-energy distributions of the ion and neutral reactants before comparison to the experimental data.[53]

For metal clusters, it has been shown that lifetime effects become increasingly important as the size of the cluster increases.[34] This is because metal clusters have many low-frequency vibrational modes such that the lifetime of the transient intermediate can exceed the experimental time available for reaction (approximately 10^{-4} s in our apparatus). Thus, an important component of the modeling of these reactions is to include the effect of the lifetime of the reaction, as estimated using statistical Rice–Ramsperger–Kassel–Marcus (RRKM) theory.[61–63]

The method to incorporate lifetime effects in our modeling has been discussed in detail previously[64] and requires molecular constants for the energized molecule (EM) and transition state (TS) leading to the products, and the reaction degeneracy (two for loss of D from the $Ni_nD_2^+$ intermediate). For the primary reaction leading to Ni_nD^+, the energized molecule is the transiently formed $Ni_nD_2^+$ complex, which we assume has a DNi_nD^+ structure. For all species, the $3n-6$ vibrations associated with the metal cluster are assumed to equal those of the bare cluster and are estimated using the elastic cluster model.[58] For DNi_nD^+, six additional frequencies are needed and are based on the experimental values of the vibrational frequencies reported for chemisorbed hydrogen on bulk nickel surfaces. For the symmetric stretching mode of H in a threefold site on a Ni(111) surface, electron energy loss measurements[65,66] give frequencies of 1122 and 1170 cm^{-1}, whereas 1137 cm^{-1} was obtained using a neutral inelastic scattering method.[67] The average of these three frequencies is 1143 cm^{-1}, and we convert this to a cluster-deuteride stretching frequency of 810 cm^{-1}. The asymmetric cluster-deuteride stretching frequency can be estimated from the symmetric stretch by multiplying by $\tan(\theta/2)$, where θ is the included angle of the M–H–M bridged species.[68] An average θ value can be obtained from calculated values of the Ni–H–Ni bond angles of 71.2°, 88.0°, and 92.9° for the three most stable isomers calculated for Ni_2H.[26] This procedure yields an estimate for the asymmetric cluster-deuteride stretching frequency of 730 cm^{-1}. To obtain the wagging frequency for DNi_nD^+, we use the ratio of symmetric stretching frequencies for DFe_nD^+ (950 cm^{-1})[45] and for DNi_nD^+ (810 cm^{-1}). This ratio (0.85) is used to scale the average value of the wagging frequency for DFe_nD^+,[45] which gives 620 cm^{-1} for the wagging frequency of DNi_nD^+. Although this procedure may be oversimplified, the magnitudes of the errors associated with these estimates of frequencies were evaluated by scaling all frequencies by ±50%, which produces differences in the thresholds that are less than 0.04 eV.

Formation of Ni_nD^+ products from the $Ni_nD_2^+$ intermediate probably occurs via a loose transition state (LTS) located at the centrifugal barrier, which is treated variationally as described in detail elsewhere.[64] For ion-molecule reactions having no barriers in excess of the reaction endothermicity, this phase space limit (PSL) is a reasonable assumption.[61] For a PSL LTS, the frequencies needed are simply those of the products, i.e., $Ni_nD^+ + D$. However, covalent bond cleavage may be better represented by a tighter transition state.[46,47,69] Therefore, we also considered a tight transition state (TTS) model where we simply remove the frequency corresponding to the reaction coordinate, a cluster-D stretch. These two models should provide conservative lower and upper limits to the dissociation rates for D atom loss from the $Ni_nD_2^+$ intermediates.

As discussed previously,[49] the use of RRKM theory is not entirely appropriate for species like transition metal clusters that have an appreciable density of electronic states. Unfortunately, more appropriate models are not yet available nor are there reliable means of accurately estimating the density of electronic states. Fortunately, because both reactants and products share this high density of electronic states, errors associated with neglecting these states should largely cancel.

Modeling of the Ni_nD^+ product cross sections includes energies above the point where the cross section declines as a result of product dissociation reaction. Including this region in our data analysis is advantageous because the more extensive energy range helps constrain the parameters in Eq. (1). This dissociation process can be modeled using simple statistical assumptions that are outlined elsewhere[70] and have been used successfully to describe the high-energy behavior of the $Ni^+ + D_2 \rightarrow NiD^+ + D$ reaction.[71] Briefly, Eq. (1) is multiplied by an energy dependent probability factor for product dissociation that depends on two adjustable parameters: E_D, the dissociation energy, and p, an empirical fitting parameter. For the reactions considered here, E_D is just the D_2 dissociation energy. Values of p ranging from 1 to 5 were tested and a value of $p = 4$ was found to best reproduce the data for most of the clusters.

IV. RESULTS

Figure 1 shows the cross sections for reaction of Ni_n^+ ($n = 2-16$) with D_2 as a function of kinetic energy over a range of thermal to as high as 8 eV (eventually limited by

1000 eV lab). Despite a careful search for products with fewer nickel atoms, the only products observed were those formed in reactions (2) and (3).

$$Ni_n^+ + D_2 \rightarrow Ni_nD^+ + D, \quad (2)$$

$$\rightarrow Ni_nD_2^+ . \quad (3)$$

Only reaction (2) is observed for clusters with $n=2-4$ atoms, whereas both reactions are observed for clusters with $n \geq 5$ atoms. Similar to our results for reactions of vanadium,[87] chromium,[46] and iron[45] cluster ions with D_2, we fail to observe collision-induced dissociation of the nickel cluster ions with D_2. These observations can be explained by previous work in our laboratory that has shown that CID processes are inefficient for target gases (like D_2) with low masses and polarizabilities.[72,73] Also, we observed no products with fewer nickel atoms than the reactants, such as $Ni_{n-1}D_2^+$ or $Ni_{n-1}D^+$. This indicates that the $Ni_nD_2^+$ and Ni_nD^+ products decompose preferentially by loss of D_2 or D, respectively, rather than Ni atom loss.

A. Cross sections for Ni_nD^+ formation

The formation of Ni_nD^+ in reaction (2) is observed to be endothermic for all clusters studied, Fig. 1. The kinetic-energy dependences of the cross sections are similar to those previously reported for V_n^+, Cr_n^+, and Fe_n^+ clusters reacting with D_2.[45–47] The cross sections exhibit apparent thresholds of 2.0 ± 0.6 eV for all clusters and reach maxima at 4–6 eV. The decline in the formation of Ni_nD^+ at elevated energies can be attributed to the overall reaction (4),

$$Ni_n^+ + D_2 \rightarrow Ni_nD^+ + D \rightarrow Ni_n^+ + 2D, \quad (4)$$

which can begin at $D_0(D_2)=4.56$ eV.[74] Smaller clusters exhibit an onset for this reaction close to its thermodynamic limit, 4.56 eV minus the internal energy of the cluster reactants. Figure 1 shows that the cross-section maximum moves to higher energies as the cluster size increases, which can be attributed to kinetic shifts in this process. Larger clusters are able to accommodate more excess energy, so that the lifetime of the Ni_nD^+ product increases with increasing cluster size and eventually becomes larger than the 10^{-4} s time window available for dissociation in our experimental apparatus. At higher kinetic energies, the lifetime for dissociation becomes shorter than this time window and the dissociation process is again observed as declines in the Ni_nD^+ cross sections. Note that the observation of maxima in the Ni_nD^+ cross sections corresponding to reaction (4) is consistent with the failure to observe Ni_mD^+ products where $m<n$, i.e., Ni_nD^+ clusters preferentially dissociate by losing D rather than Ni atoms. Qualitatively, this result shows that Ni_n^+–D bonds are weaker than DNi_{n-1}^+–Ni bonds.

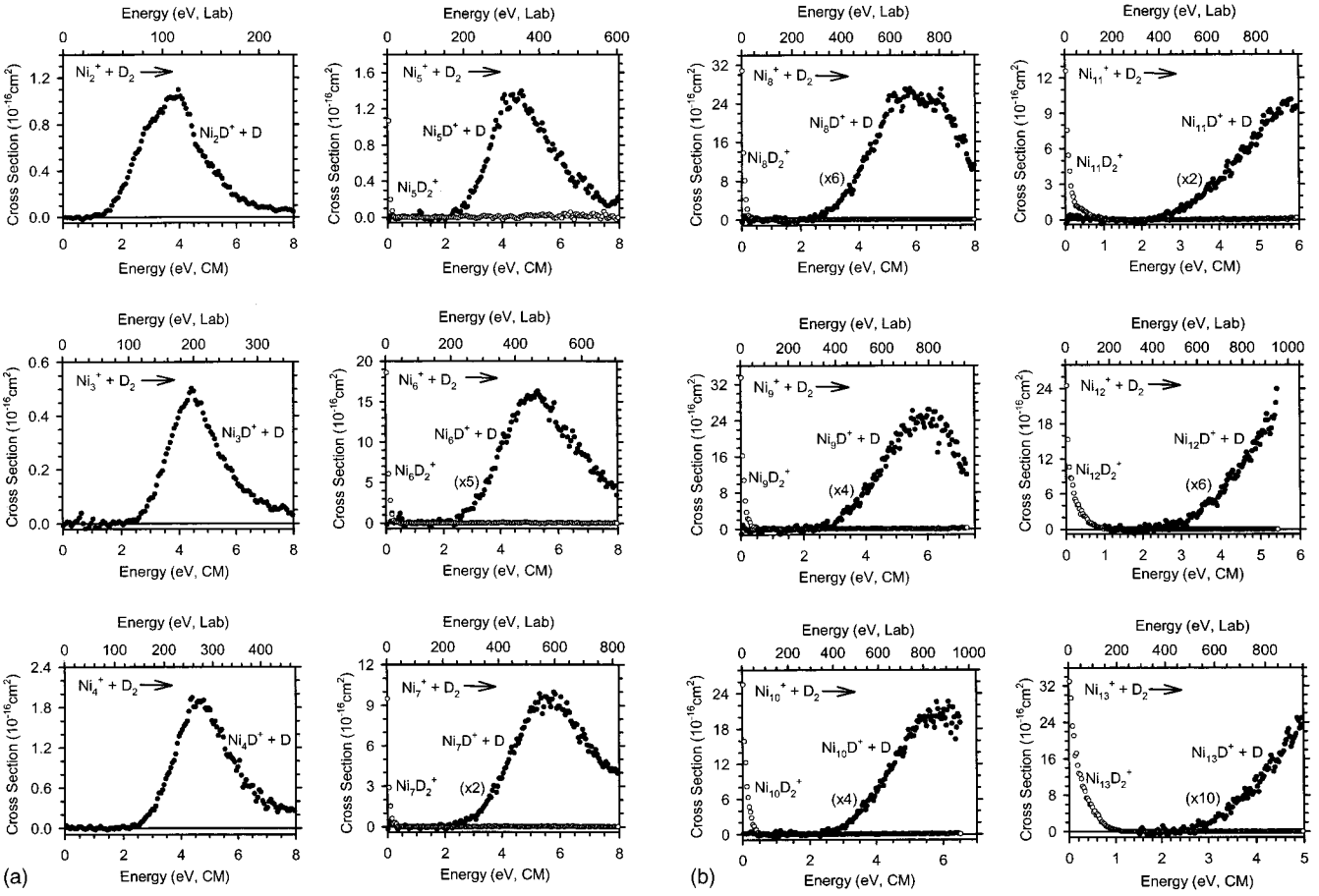

FIG. 1. Cross sections for reactions of Ni_n^+ ($n=2-16$) with D_2 as a function of collision energy in the center-of-mass (lower x-axis) and laboratory (upper x-axis) frames.

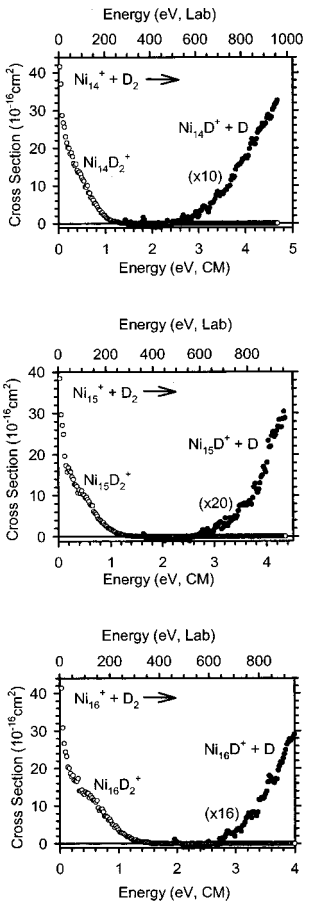

FIG. 1. (*Continued.*)

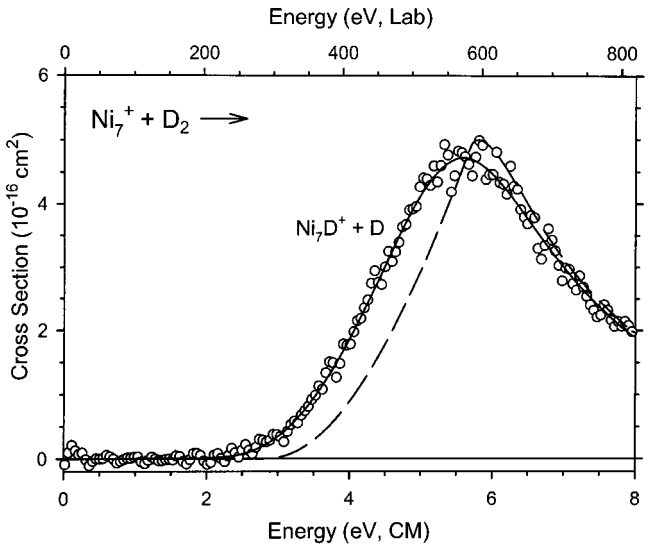

FIG. 2. Cross section for reaction (2) with $n=7$ as a function of collision energy in the center-of-mass (lower x-axis) and laboratory (upper x-axis) frames. The dashed line shows the model of Eq. (1) with optimized parameters from Table I along with model for product dissociation. The analysis shown includes both internal energy and RRKM lifetime effects and the onset for product dissociation was set to D_2 bond dissociation energy, 4.56 eV. The solid line shows the model after convolution over the neutral and ion kinetic-energy distribution.

B. Ni_n^+–D thresholds

The optimum values of the parameters of Eq. (1), E_0, σ_0, and N, used to reproduce the cross sections for the monodeuteride products are given in Table I. Ni_nD^+ product cross sections are modeled using both loose (phase space limit, PSL) and tight transition states, as described previously. A representative fit of data for the monodeuteride product ions is shown in Fig. 2. Thresholds measured in these experiments can be used to derive bond energies of Ni_n^+–D by assuming that there are no barriers to reaction (2) in excess of the endothermicity. This assumption has proved to be valid for many ion-molecule reactions because the

TABLE I. Summary of parameters used in Eq. (1) for the analysis of Ni_nD^+ cross sections.[a]

n	σ_0[b]	N[b]	E_0 (TTS)[c] eV	E_0 (PSL)[d] eV	D_0 (Ni_n^+–D)[e] eV
1		1.1 (0.1)[f]		2.84 (0.04)[f]	1.72 (0.08)[f]
2	1.7 (0.2)	1.2 (0.2)	1.52 (0.09)	1.52 (0.10)	3.04 (0.10)
3	1.2 (0.1)	1.7 (0.2)	2.55 (0.08)	2.58 (0.08)	2.00 (0.10)
4	4.1 (0.6)	1.6 (0.2)	2.56 (0.09)	2.68 (0.10)	1.94 (0.16)
5	3.0 (0.3)	1.6 (0.2)	2.39 (0.07)	2.56 (0.06)	2.09 (0.15)
6	3.1 (0.4)	1.8 (0.1)	2.18 (0.06)	2.42 (0.07)	2.26 (0.19)
7	3.7 (1.0)	2.0 (0.3)	2.22 (0.15)	2.48 (0.15)	2.21 (0.28)
8	7.6 (2.3)	1.4 (0.3)	2.23 (0.18)	2.72 (0.19)	2.10 (0.41)
9	6.7 (1.3)	1.7 (0.2)	2.10 (0.10)	2.54 (0.13)	2.24 (0.34)
10	4.9 (0.9)	1.8 (0.2)	1.91 (0.08)	2.38 (0.10)	2.42 (0.33)
11	3.1 (1.0)	2.0 (0.2)	1.70 (0.13)	2.16 (0.17)	2.63 (0.38)
12	3.1 (0.6)	2.0 (0.1)	1.83 (0.09)	2.33 (0.11)	2.48 (0.35)
13	2.6 (0.3)	1.9 (0.1)	1.71 (0.07)	2.22 (0.09)	2.60 (0.34)
14	5.0 (0.7)	1.9 (0.1)	1.67 (0.08)	2.18 (0.09)	2.64 (0.34)
15	4.8 (0.6)	2.0 (0.1)	1.73 (0.09)	2.29 (0.11)	2.55 (0.38)
16	8.5 (1.8)	1.9 (0.1)	1.62 (0.09)	2.16 (0.11)	2.67 (0.37)

[a]Uncertainties in parentheses.
[b]Values for LTS model. TTS parameters are similar.
[c]Tight transition state (TTS) model described in text.
[d]Loose transition state phase-space limit (PSL) model described in text.
[e]Average value derived from TTS and PSL thresholds according to Eq. (5).
[f]Value from Ref. 71.

long-range ion-induced dipole interactions between ions and polarizable neutrals are attractive. Exceptions often involve restrictions in spin or orbital angular momentum.[56,75] Unfortunately, conservation of such quantities cannot be examined for the present systems because detailed information concerning the electronic states of both reactants and products are not available. However, transition metal clusters have a dense manifold of electronic states, such that interactions (such as spin–orbit mixing) among these surfaces should allow adiabatic pathways for product formation without barriers in the excess of the endothermicities for Ni_nD^+. Thus, we assume the thresholds for reactions leading to the formation of Ni_nD^+ represent the adiabatic endothermicities.

Given the assumption that there are no barriers in excess of the endothermicities to the formation of $Ni_nD^+ + D$, the thresholds for reaction (2), E_0, can be converted to $Ni_n^+ - D$ bond energies according to Eq. (5):

$$D_0(Ni_n^+ - D) = D_0(D_2) - E_0. \quad (5)$$

Because the model of Eq. (1) explicitly accounts for the internal energy and translational energy distributions of the reactants, the thermochemistry derived corresponds to 0 K. Bond energies calculated in this manner are given in Table I, as an average of values derived from thresholds obtained using kinetic shifts modeled with loose (PSL) and tight TS assumptions.

C. Cross sections for $Ni_nD_2^+$ formation

The smallest cluster for which a dideuteride product is observed is Ni_5^+. The cross sections for all observed dideuteride products, $Ni_nD_2^+$, decrease monotonically with increasing energy, as shown in Figs. 1 and 3. This behavior is characteristic of exothermic ion-molecule reactions. In addition, the magnitudes of the cross sections for $Ni_nD_2^+$ generally increase as the cluster size increases in the low-energy range except for $Ni_7D_2^+$ and $Ni_{11}D_2^+$. The cross sections decline roughly as $E^{-1/2}$ at lower energies, although the data point density for $Ni_5D_2^+$ cluster is too low to ascertain the dependence confidently. Such behavior conforms to the $E^{-1/2}$ energy dependence predicted for ion-molecule collisions by the Langevin–Gioumousis–Stevenson (LGS) model.[76] The cross-section magnitudes for $Ni_nD_2^+$ ($n = 13-16$) are very close to, but about half of the LGS model prediction at the lower energies.

With increasing interaction energy, the magnitudes of all $Ni_nD_2^+$ cross sections decline more rapidly. These declines of the exothermic $Ni_nD_2^+$ product cross sections with increasing energy can be attributed to the overall reaction (6), as no other dissociation process is energetically accessible.

$$Ni_2^+ + D_2 \rightarrow Ni_nD_2^+ \rightarrow Ni_n^+ + D_2. \quad (6)$$

No energy is required for this overall process as the products are the same as the initial reactants. We believe that the more rapid decline in the cross sections can be attributed to the changing lifetime of the intermediate, which decreases as the interaction energy increases and increases with cluster size. Observation of the $Ni_nD_2^+$ product is expected only if its lifetime exceeds or is on the order of the detection time window of our instrument, $\sim 10^{-4}$ s. The reason that we do not observe any $Ni_nD_2^+$ products for $n < 5$ is probably because smaller clusters $Ni_nD_2^+$ dissociate more rapidly than this, even at low kinetic energies.

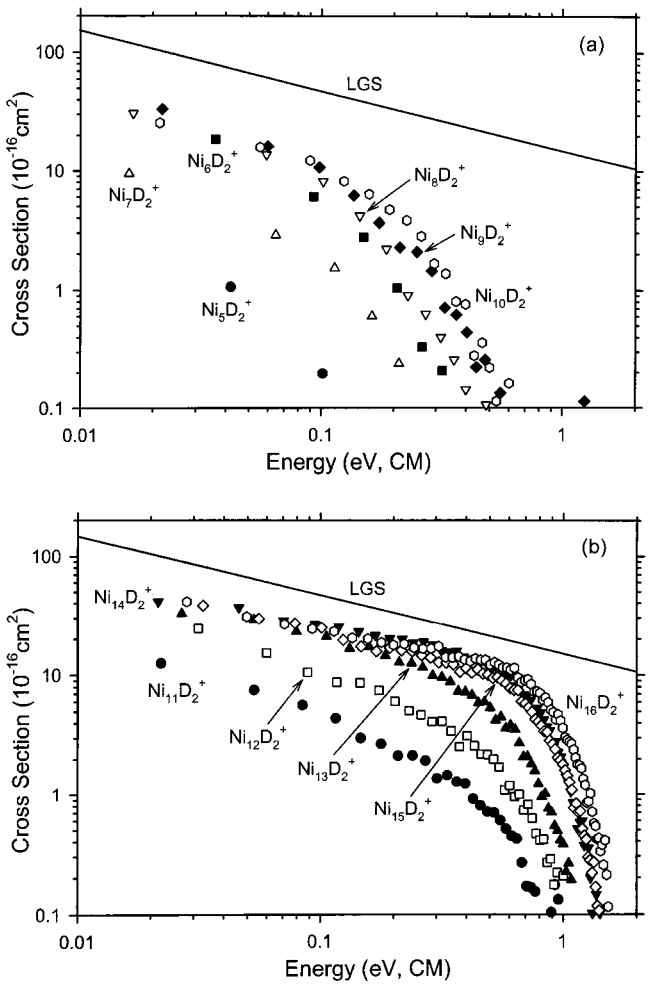

FIG. 3. Cross sections for reaction (3) plotted on a log scale for $n = 5-16$ as a function of collision energy in the center-of-mass frame. The solid line indicates the LGS model cross section (Ref. 76).

The $Ni_nD_2^+$ product ion can conceivably have one of two forms: (1) a weakly bound adduct held together by the ion-induced dipole attraction, i.e., a physisorbed state; or (2) a strongly bound chemisorbed species where both deuterium atoms are chemically bonded to the cluster, i.e., a dissociative chemisorbed state. We have previously argued[45–47] that a weakly bound adduct in which the D_2 molecule was intact should allow reaction (6) to be kinetically facile as well as being thermodynamically allowed at all collision energies. Consequently, it is difficult to understand how such a weakly bound physisorbed species can survive our instrumental flight time of 10^{-4} s, unless it is collisionally stabilized by multiple collisions with D_2. Our pressure dependent studies verify that the $Ni_nD_2^+$ products are not the result of collision stabilization. Therefore, formation of $Ni_nD_2^+$ products does not behave as expected for physisorbtion processes. However, if the $Ni_nD_2^+$ clusters are dissociatively chemisorbed species, then reaction (6) requires that the two deuterium atoms come back together and pass through a tight transition

TABLE II. Thermal rate constants (10^{-10} cm^3/s) for reactions of nickel clusters with D_2.

	Experiments				Theory	
n	This work[a]	Ref. 11[b]	Ref. 12[c]	Ref. 13[c]	Ref. 20	Ref. 21[d]
3		3.8				
4		2.0				
5	0.15	3.0				
6	2.3	2.3				
7	0.80	3.0	1.2		2.5	2.68
8	3.3	2.6	0.8		2.8	2.86
9	2.9	3.6	0.1	0.4	3.2	3.67
10	3.1	3.6	3.0	4.0	3.6	3.80
11	1.6	3.3	2.4	4.0		3.93
12	3.7	5.1	2.5	5.7		4.46
13	5.0	6.6	4.2	9.0	3.0	5.20
14	5.8	5.7	2.5	8.1	5.5	5.76
15	6.2	6.2	3.0			
16	5.5	8.0	2.9			
17		6.2	2.6			
18		8.2	2.7			
19		8.1	3.3		6.4	6.83
20		9.0	3.9			

[a]Rate constants for reaction of nickel cation clusters, Ni_n^+, with D_2 measured here under single collision conditions. Uncertainties are ±30%.
[b]Relative rate constants for reaction of neutral nickel clusters Ni_n with D_2, scaled to the value for Ni_{10}, see text. Estimated error bounds are ±20%.
[c]Absolute rate constants for reaction of neutral nickel clusters, Ni_n, with D_2. The accuracy of the rate constants is ±50%.
[d]At $T=0$ K.

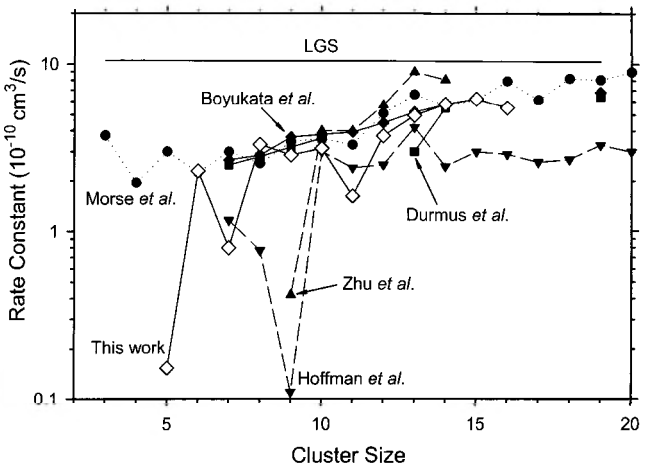

FIG. 4. Rate constants for nickel cluster reactions with D_2 at thermal energy. Open diamonds and full lines indicate our experimental values on nickel cluster cations. Experimental values for neutral nickel clusters are indicated by solid triangles and dashed lines (Refs. 12 and 13) and solid circles and dotted lines (relative rate constants from Ref. 11, scaled to the value for Ni_{10}). Solid squares and full lines ($T=0$ K, Ref. 20) and solid diamonds and full lines (Ref. 21) indicate theoretical values for neutral nickel clusters. The horizontal line indicates the LGS value for the collision rate constant (Ref. 76).

state associated with cleaving the cluster-deuterium bonds and forming a D_2 bond. Such a process should be kinetically hindered, especially for larger clusters where the chemisorbtion energy can be dissipated throughout the cluster. This would explain the long lifetimes observed for $Ni_nD_2^+$ ($n \geq 5$) products and why the magnitudes of the $Ni_nD_2^+$ cross sections increase for larger clusters. Clearly, chemisorbtion is efficient for the larger clusters.

D. Rate constants for $Ni_nD_2^+$ formation

Reaction rate constants can be obtained from our cross sections by using the expression, $k(\langle E\rangle)=\nu\sigma(E)$ where $\nu=(2E/\mu)^{1/2}$ and $\mu=mM/(m+M)$, the reduced mass of the reactants. The rate constants depend on the mean energy of the reactants, which includes the average thermal motion of the neutral, such that $\langle E\rangle=E+(3/2)\gamma k_BT$ where $\gamma=M/(m+M)$. Table II and Fig. 4 show our absolute rate constants for reactions of nickel cation clusters Ni_n^+ with D_2 to form $Ni_nD_2^+$ at single collision conditions and thermal energies. In general, odd-even oscillations are observed for clusters sizes $n=5-11$, with rate constants of odd-sized cation clusters being smaller than those of adjacent even-sized cation clusters. Similar odd-even oscillations in rate constants and reactivity have been found for reactions of vanadium[47,77,78] and chromium[46] cation clusters with D_2. Interestingly, as for nickel, the even-sized chromium clusters are more reactive, whereas the odd-sized vanadium clusters are more reactive. These patterns have been interpreted to indicate that the more reactive clusters have open-shell character with regard to the molecular orbitals formed from the atomic 4s orbitals. A similar conclusion seems warranted for nickel clusters as well. For reactions of Ni_n^+ ($n \geq 12$), the rate constants increase with cluster sizes leveling out for $n=14-16$. In general, our experimental results average about half the LGS value[76] of 10.4×10^{-10} cm^3 s^{-1} for $n=8-16$.

Although the rates of neutral and cationic nickel clusters reaction with D_2 need not be identical, it is of interest to make such a comparison. Figure 4 and Table II compare our rate constants with the results from previous work[11–13,20,21] on the reaction of neutral nickel clusters with D_2. Experimental values for neutral nickel clusters measured by Hoffman *et al.*[12] and Zhu *et al.*[13] both used the same experimental flow tube reactor to measure rates, but differ in the method of determining the absolute rate constants, with the latter study being more accurate. Relative values from Morse *et al.*[11] are compared to the others by scaling these to the value of Ni_{10}, chosen because of the good agreement between the theoretical and experimental absolute values (Fig. 4). Theoretical results obtained using molecular dynamics simulations are available from Durmus *et al.*[20] and Boyukata *et al.* ($T=0$ K).[21] In agreement with our observations for the cationic clusters, reaction rates for neutral nickel clusters generally increase with cluster size. Our results for larger nickel cluster cations ($n \geq 10$) are in reasonable agreement with the absolute experimental and theoretical values. For smaller clusters ($n \leq 9$), there are clear differences between the results, which indicate that the differing electronic and possibly geometric structures of the neutral and cationic clusters influences the observed reactivity.

V. DISCUSSION

A. Comparison of D_2 activation by Ni^+ and Ni_n^+

The cross section for the reaction of D_2 with atomic nickel ion in its electronic ground state, $Ni^+(^2D,3d^9)$,

reaches a maximum of $\sim 0.18\times10^{-16}$ cm^2 for reaction (2).[71] The first excited state of atomic nickel ions, $Ni^+(^4F,4s3d^8)$, reacts inefficiently with D_2, forming NiD^+ with a maximum cross section of only about 0.06×10^{-16} cm^2. The lower efficiency of the first excited state $Ni^+(^4F,4s3d^8)$ can be rationalized in terms of a repulsive interaction between the σ-bonding electrons of D_2 and the $4s$ electron on the nickel ion. For the ground state $Ni^+(^2D,3d^9)$, this repulsive interaction is absent because the $4s$ orbital is empty, such that the D_2 molecule can approach the metal center more closely. At such distances, D_2 activation is achieved by donation of the D_2 bonding electrons into the empty $4s$ metal orbital and back donation of metal $3d\pi$ electrons to the σ^* antibonding orbital of D_2.

A comparison of the reaction cross sections for $Ni^+ + D_2$ and our present results can provide insights into the interactions between the cluster ions and D_2. The absolute magnitudes of the reaction cross sections for Ni_n^+ are larger than that for ground state $Ni^+(^2D,3d^9)$ by factors ranging from 6 ($n=2$) to 30 ($n=10$). In general, the magnitudes of the reactions increase with increasing cluster size, consistent with larger collision cross sections for the physically larger clusters. This indicates that the electronic requirements necessary for the reaction of D_2 with Ni_n clusters are similar or enhanced compared to those for $Ni^+(^2D,3d^9)$. Thus cluster orbitals of appropriate symmetries and occupancies are available to interact with the σ and σ^* orbitals of D_2.[79,80]

B. Ni_n^+–D bond energies

Table I lists the thresholds derived from analysis of the Ni_nD^+ cross sections using Eq. (1), assuming both loose and tight transition states. Both sets of energies show the same oscillations with cluster size n. Relative to the TTS values, thresholds obtained using the PSL model are the same for Ni_2^+ and Ni_3^+, and then gradually increase. They are an average of 0.22 ± 0.10 eV higher than the TTS values for $n=4-7$, and 0.50 ± 0.06 eV for $n\geq8$.

Because we do not know the nature of the transition state definitely, we conservatively take our best values for the Ni_n^+–D bond energies as those derived using Eq. (1) from the average of the TTS and PSL threshold energies. The loose and tight transition state models provide conservative lower and upper limits to the bond dissociation energy. These average Ni_n^+–D bond energies are listed in Table I and shown in Fig. 5 along with uncertainties increased to reflect the span of values. It should be noted that the listed uncertainties reflect the absolute accuracy of each individual determination. Relative uncertainties, especially for adjacent cluster sizes, should be substantially smaller, probably on the order of 0.1 eV or less, because systematic errors in the interpretations cancel.

The accuracy of these values can be qualitatively assessed by two considerations. First, we observe that Ni_nD^+ products decompose by losing D atoms, rather than Ni atoms. This shows that $D(Ni_n^+-D)$ should be less than $D(DNi_{n-1}^+-Ni)$. The latter quantity can be equated with $D(Ni_{n-1}^+-Ni)+D(Ni_n^+-D)-D(Ni_{n-1}^+-D)$, which means that if the bond energies, $D(Ni_n^+-D)$, are less than

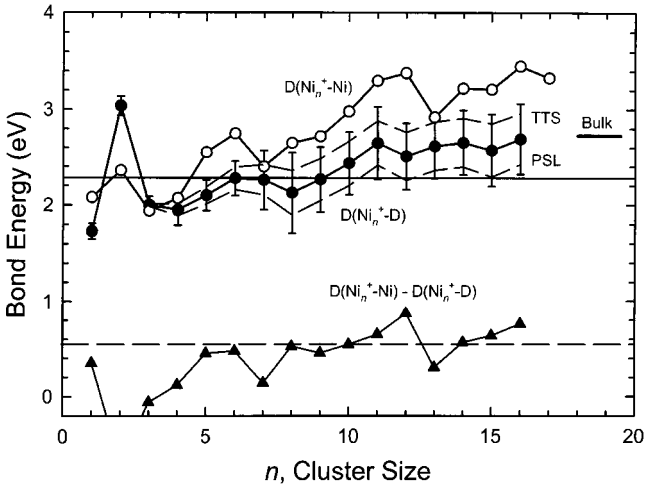

FIG. 5. $D_0(Ni_n^+-D)$ (●, Table I), $D_0(Ni_n^+-Ni)$ (○, Ref. 36), and the difference, $D_0(Ni_n^+-Ni)-D_0(Ni_n^+-D)$ (▲), plotted as a function of cluster size, n. The horizontal solid line at 2.28 eV indicates half of the $D_0(D-D)$ bond energy. The two dashed lines indicate the upper and lower limits to the Ni_n^+-D bond energies obtained by analysis using PSL and TTS models. The small horizontal solid line labeled bulk indicates the average of the experimental binding energies of H to Ni(111), Ni(100), and Ni(110) surfaces (Ref. 29, 90, and 91).

$D(DNi_{n-1}^+-Ni)$, then $D(Ni_{n-1}^+-Ni)$ are larger than $D(Ni_{n-1}^+-D)$. From Fig. 5, it can be seen that $D(Ni_{n-1}^+-Ni)$ are larger than our measured values of $D(Ni_{n-1}^+-D)$ in all cases but $n=3$, $D(Ni_2^+-D)>D(Ni_2^+-Ni)$. Values for $n=4$ are within experimental errors. Thus, the average $D(Ni_n^+-D)$ values except for $n=3$ are qualitatively consistent with the decomposition patterns observed for these products.

Second, we consider our observation of dissociative chemisorbtion of D_2 on the clusters. These chemisorbed $Ni_nD_2^+$ species are formed exothermically for clusters where $n\geq5$, indicating that $D_0(DNi_n^+-D)+D_0(Ni_n^+-D)>4.56$ eV $=D_0(D_2)$. Assuming that the first and second cluster-deuterium bonds are roughly comparable, we should observe exothermic formation of $Ni_nD_2^+$ when $D_0(Ni_n^+-D)\geq D_0(D_2)/2=2.28$ eV, indicated by a line in Fig. 5. As can be seen from Table I and Fig. 5, the average $D(Ni_n^+-D)$ values exceed this energy for $n\geq10$ and values for $n=5-9$ are very close to this energy (within the uncertainty of the measurement). This is in qualitative agreement with our observation of $Ni_nD_2^+$ products at thermal energies for the $n\geq5$ clusters. This criterion tends to suggest that the higher TTS values are more accurate than the loose PSL value.

C. Comparison of $D(Ni_n^+-D)$ and $D(Ni_n^+-Ni)$

Figure 5 compares the cluster-deuteride bond energies derived in this study with metal–metal bond energies determined previously.[36] Overall, both $D_0(Ni_n^+-D)$ and $D_0(Ni_n^+-Ni)$ generally increase as the cluster size increases, and they parallel one another for many cluster sizes. This can be rationalized by noting that the number of neighboring atoms increases quickly over this cluster size range so that dissociation requires cleavage of more metal-deuteride and metal–metal bonds. However, the increase is nonmonotonic

with local maxima at Ni_2^+–D, Ni_6^+–D, and Ni_{11}^+–D for nickel-deuteride ionic clusters, and at Ni_2^+–Ni, Ni_6^+–Ni, and Ni_{12}^+–Ni for pure metal clusters. As noted above, $D_0(Ni_n^+-D)$ are weaker than $D_0(Ni_n^+-Ni)$, except for $n=2$ and 3. This is more easily seen from the difference of the bond energies, $D_0(Ni_n^+-Ni)-D_0(Ni_n^+-D)$, also plotted as a function of cluster size n in Fig. 5.

As the bonding in the Ni_n^+–D systems must involve the $1s$ electron on deuterium, the parallel bond energies in Ni_n^+–Ni cluster systems suggest that the bonding is predominantly $4s$-$4s$. The metal–metal bonds are an average of about 0.56 ± 0.10 eV stronger than metal-deuterium bonds for $n=5$, 6, 8–11, and 14–16. This increase means that metal bonds can be enhanced by using $3d$-$3d$ interactions. For $n=12$, the difference in bond energies is 0.87 eV. We speculate that there may be geometric contribution to the bond energy variation. In analogy with our observations for iron,[45] chromium,[46] and vanadium[47] clusters, this suggestion relies on the strong possibility that Ni_{13}^+ (icosahedral or octahedral with fcc or bcc packing) can have a highly symmetric geometrical structure compared to neighboring clusters. Substitution of D for Ni in Ni_{13}^+ cluster breaks the symmetry, changing the molecular orbital ordering, thereby leading to a less strongly bound system. For several other clusters, $n=3$, 4, 7, and 13, the average difference in bond energies is small, 0.16 ± 0.09 eV. These clusters are less stable compared to their neighbors, as can be seen from the absolute bond energies, $D(Ni_n^+-Ni)$, which reach local minima at these sizes. The comparison with the $D(Ni_n^+-D)$ bond energies suggests that Ni_4^+, Ni_5^+, Ni_8^+, and Ni_{14}^+ clusters do not utilize $3d$-$3d$ bonding as efficiently as their neighbors.

Although the comparison between $D_0(Ni_n^+-Ni)$ and $D_0(Ni_n^+-D)$ shows that $D_0(Ni_n^+-Ni)$ are generally stronger than $D_0(Ni_n^+-D)$ for most cluster sizes, there is a clear exception. $D_0(Ni_2^+-D)$ is 0.68 eV larger than $D_0(Ni_2^+-Ni)$, although both bond energies are local maxima in their respective series. Because there is so little known about the geometric and electronic structures of nickel cation clusters, we are left to speculate regarding a possible explanation. Nickel atoms have two nearly degenerate electronic states, $^3D(4s3d^9)$, and the ground state, $^3F(4s^23d^8)$, with an energy difference of only 0.03 eV between the lowest spin–orbit levels.[81] When the other spin–orbit levels of these states are explicitly included, the average energy ordering actually changes such that the ^3D state is 0.03 eV below the ^3F state. Small nickel clusters are generally considered to be formed most readily from nickel atoms in their $4s3d^9$ configurations,[36,82,83] where the $3d^9$ cores are essentially nonbonding and localized on each atom. Using such a model, we have previously speculated that the Ni_3^+ trimer can be formed by combining ground-state $Ni^+(^2D,3d^9)$ with 2 $Ni(^3D,4s3d^9)$ to yield a species with only two $4s$ electrons. The Ni_3^+ trimer cluster has a likely near-equilateral triangle structure with an electronic stability relative to its neighbors driven by the equality of the three metal centers. Likewise, it seems reasonable that the deuterium atom in Ni_2D^+ is in a bridging position (as calculated for the neutral Ni_2D analogue),[26] but the electron density is no longer shared equally by the three centers. Apparently, this electronic distribution permits the formation of a much stronger bond, which disappears as soon as further nickel atoms are available. Quantum chemical calculations on these small nickel cluster cations and their deuterated analogues would be of clear interest in understanding why this occurs. Such understanding may provide further insight into the results of calculations that indicate that hydrogen atoms in bridging positions are less strongly bound than those in three-fold sites on bulk nickel surfaces.[84–89]

D. Comparisons to bulk phase thermochemistry

It is very interesting to compare the thermochemistry determined here with values from surface science. Experimental values for the binding of hydrogen on Ni(111) are 2.70[90] and 2.74 eV,[29,91] 2.74 eV on Ni(100),[29] and 2.70 eV on Ni(110).[29] Calculated hydrogen binding energies on (111), (100), and (110) fcc and hcp nickel surfaces are 2.56–2.91 eV,[84–89] 2.66–2.79 eV,[84–86] and 2.71–2.75 eV,[84–86] respectively, in reasonable agreement with the experimental values. The average experimental value, 2.72 eV, is plotted in Fig. 5, where it can be seen that the Ni_n^+–D bond energies for larger clusters ($n\geq11$) are very close to that for bulk phase nickel. Similar observations have been made for V_n^+–D,[47] Cr_n^+–D,[46] Fe_n^+–D,[45] V_n^+–O,[42] Cr_n^+–O,[41,44] and Fe_n^+–O[40,43] bond energies. This indicates that chemical binding is largely a local phenomenon as long as clusters have enough electronic "flexibility" to form strong covalent bonds.

ACKNOWLEDGMENTS

This work is supported by the Chemical Sciences, Geosciences, and Biosciences Division, Office of Basic Energy Sciences, Office of Science, U.S. Department of Energy. The author F. L. thanks X.-G. Zhang, J. Amicangelo, and H. Koizumi for helpful discussions.

[1] M. D. Morse, Chem. Rev. **86**, 1049 (1986); M. M. Kappes, *ibid.* **88**, 372 (1988); D. C. Parent and S. L. Anderson, *ibid.* **92**, 1541 (1992).
[2] M. P. Irion, Int. J. Mass Spectrom. Ion Processes **121**, 1 (1992).
[3] P. B. Armentrout, J. B. Griffin, and J. Conceição, in *Progress in Physics of Clusters*, edited by G. N. Chuev, V. D. Lakhno, and A. P. Nefedov (World Scientific, Singapore, 1999), p. 198; P. B. Armentrout, Annu. Rev. Phys. Chem. **52**, 423 (2001).
[4] J. Conceição, R. T. Laaksonen, L.-S. Wang, T. Guo, P. Nordlander, and R. E. Smalley, Phys. Rev. B **51**, 4668 (1995).
[5] P. Fayet, M. J. McGlinchey, and L. H. Wöste, J. Am. Chem. Soc. **109**, 1733 (1987).
[6] S. Vajda, S. Wolf, T. Leisner, U. Busolt, and L. H. Wöste, J. Chem. Phys. **107**, 3492 (1997).
[7] M. Ichihashi, T. Hanmura, R. T. Yadav, and T. Kondow, J. Phys. Chem. A **104**, 11885 (2000).
[8] E. K. Parks, K. P. Kerns, and S. J. Riley, J. Chem. Phys. **112**, 3384 (2000).
[9] K. P. Kerns, E. K. Parks, and S. J. Riley, J. Chem. Phys. **112**, 3394 (2000).
[10] P. A. Hintz and K. M. Ervin, J. Chem. Phys. **100**, 5715 (1994).
[11] M. D. Morse, M. E. Geusic, J. R. Heath, and R. E. Smalley, J. Chem. Phys. **83**, 2293 (1985).
[12] W. F. Hoffman, III, E. K. Parks, G. C. Nieman, L. G. Pobo, and S. J. Riley, Z. Phys. D: At., Mol. Clusters **7**, 83 (1987).
[13] L. Zhu, J. Ho, E. K. Parks, and S. J. Riley, J. Chem. Phys. **98**, 2798 (1993).
[14] E. K. Parks, G. C. Nieman, L. G. Pobo, and S. J. Riley, J. Phys. Chem. **91**, 2671 (1987).
[15] T. D. Klots, B. J. Winter, E. K. Parks, and S. J. Riley, J. Chem. Phys. **95**, 8919 (1991).
[16] E. K. Parks, G. C. Nieman, and S. J. Riley, Surf. Sci. **355**, 127 (1996).

[17] E. K. Parks, G. C. Nieman, and S. J. Riley, J. Chem. Phys. **115**, 4125 (2001).
[18] J. Jellinek and Z. B. Güvenç, Z. Phys. D: At., Mol. Clusters **19**, 371 (1991); J. Jellinek and I. L. Garzón *ibid.* **20**, 239 (1991); J. Jellinek and Z. B. Güvenç, *ibid.* **26**, 110 (1993).
[19] J. Jellinek and Z. B. Güvenç, in: *Topics in Atomic and Nuclear Collisions*, edited by B. Remaund (Plenum, New York, 1994), p. 243; in: *The Synergy Between Dynamics and Reactivity at Clusters and Surfaces*, edited by L. J. Farrugta (Kluwer, Dordrecht, 1995), p. 217.
[20] P. Durmuş, M. Böyükata, S. Özçelik, Z. B. Güvenç, and J. Jellinek, Surf. Sci. **454**, 310 (2000).
[21] M. Böyükata, Z. B. Güvenç, S. Özçelik, P. Durmuş, and J. Jellinek, Int. J. Quantum Chem. **84**, 208 (2001).
[22] K. Raghaven, M. S. Stave, and A. E. DePristo, Chem. Phys. Lett. **149**, 89 (1988).
[23] K. Raghavan, M. S. Stave, and A. E. DePristo, J. Chem. Phys. **91**, 1904 (1989).
[24] R. Fournier, M. S. Stave, and A. E. DePristo, J. Chem. Phys. **96**, 1530 (1992).
[25] B. Chen, M. A. Gomez, M. Sehl, J. D. Doll, and D. L. Freeman, J. Chem. Phys. **105**, 9686 (1996).
[26] E. Curotto, A. Matro, D. L. Freeman, and J. D. Doll, J. Chem. Phys. **108**, 729 (1998).
[27] B. Chen, M. A. Gomez, J. D. Doll, and D. L. Freeman, J. Chem. Phys. **108**, 4031 (1998).
[28] Y. L. Álvarez, G. E. López, and A. J. Cruz, J. Chem. Phys. **107**, 1420 (1997).
[29] K. Christmann, O. Schober, G. Ertl, and M. Neuman, J. Chem. Phys. **60**, 4528 (1974).
[30] L. Lian, C. X. Su, and P. B. Armentrout, J. Chem. Phys. **97**, 4084 (1992).
[31] C. X. Su, D. A. Hales, and P. B. Armentrout, J. Chem. Phys. **99**, 6613 (1993).
[32] C. X. Su, D. A. Hales, and P. B. Armentrout, Chem. Phys. Lett. **201**, 199 (1993).
[33] C. X. Su and P. B. Armentrout, J. Chem. Phys. **99**, 6506 (1993).
[34] L. Lian, C. X. Su, and P. B. Armentrout, J. Chem. Phys. **97**, 4072 (1992).
[35] D. A. Hales, C. X. Su, and P. B. Armentrout, J. Chem. Phys. **100**, 1049 (1994).
[36] L. Lian, C. X. Su, and P. B. Armentrout, J. Chem. Phys. **96**, 7542 (1992).
[37] D. A. Hales, L. Lian, and P. B. Armentrout, Int. J. Mass Spectrom. Ion Processes **102**, 269 (1990).
[38] P. B. Armentrout, D. A. Hales, and L. Lian, in *Advances in Metal and Semiconductor Clusters*, edited by M. A. Duncan (JAI, Greenwich, 1994), Vol. 2, p. 1.
[39] P. B. Armentrout, in *Metal-Ligand Interactions—Structure and Reactivity*, edited by N. Russo and D. R. Salahub (Kluwer, Dordrecht, 1996), p. 23.
[40] J. B. Griffin and P. B. Armentrout, J. Chem. Phys. **106**, 4448 (1997).
[41] J. B. Griffin and P. B. Armentrout, J. Chem. Phys. **108**, 8062 (1998).
[42] J. Xu, M. T. Rodgers, J. B. Griffin, and P. B. Armentrout, J. Chem. Phys. **108**, 9339 (1998).
[43] J. B. Griffin and P. B. Armentrout, J. Chem. Phys. **107**, 5345 (1997).
[44] J. B. Griffin and P. B. Armentrout, J. Chem. Phys. **108**, 8075 (1998).
[45] J. Conceicao, S. K. Loh, L. Lian, and P. B. Armentrout, J. Chem. Phys. **104**, 3976 (1996).
[46] J. Conceicao, R. Liyanage, and P. B. Armentrout, Chem. Phys. **262**, 115 (2000).
[47] R. Liyanage, J. Conceicao, and P. B. Armentrout, J. Chem. Phys. **116**, 936 (2002).
[48] R. Liyanage, X.-G. Zhang, and P. B. Armentrout, J. Chem. Phys. **115**, 9747 (2001).
[49] S. K. Loh, D. A. Hales, L. Lian, and P. B. Armentrout, J. Chem. Phys. **90**, 5466 (1989).
[50] T. G. Deitz, M. A. Duncan, D. E. Powers, and R. E. Smalley, J. Chem. Phys. **74**, 6511 (1981).
[51] S. K. Loh, D. A. Hales, and P. B. Armentrout, Chem. Phys. Lett. **129**, 527 (1986).
[52] E. Teloy and D. Gerlich, Chem. Phys. **4**, 417 (1974); D. Gerlich, Adv. Chem. Phys. **82**, 1 (1992); D. Gerlich, in *State-Selected and State-to-State Ion-Molecule Reaction Dynamics*, edited by C.-Y. Ng, and M. Baer (Wiley, New York, 1992), p. 1.
[53] K. M. Ervin and P. B. Armentrout, J. Chem. Phys. **83**, 166 (1985).
[54] N. R. Daly, Rev. Sci. Instrum. **31**, 264 (1959).
[55] W. J. Chesnavich and M. T. Bowers, J. Phys. Chem. **83**, 900 (1979).
[56] P. B. Armentrout, in *Advances in Gas Phase Metal Ion Chemistry*, edited by N. G. Adams and L. M. Babcock (JAI, Greenwich, CT, 1992), Vol. 1, p. 83.
[57] P. B. Armentrout, Int. J. Mass Spectrom. **200**, 219 (2000).
[58] A. A. Shvartsburg, K. M. Ervin, and J. H. Frederick, J. Chem. Phys. **104**, 8458 (1996).
[59] R. J. Birgenean, J. Cordes, G. Dolling, and A. D. Woods, Phys. Rev. **136**, A1359 (1964).
[60] G. Simmons and H. Wang, *Single Crystal Elastic Constants and Calculated Aggregate Properties: A Handbook*, 2nd ed. (M.I.T., Cambridge, MA, 1971).
[61] R. G. Gilbert and S. C. Smith, *Theory of Unimolecular and Recombination Reactions* (Blackwell Scientific, Oxford, 1990).
[62] K. A. Holbrook, M. J. Pilling, and S. H. Robertson, *Unimolecular Reactions*, 2nd ed. (Wiley, New York, 1996).
[63] D. G. Truhlar, B. C. Garrett, and S. J. Klippenstein, J. Phys. Chem. **100**, 12771 (1996).
[64] M. T. Rodgers, K. M. Ervin, and P. B. Armentrout, J. Chem. Phys. **106**, 4499 (1997).
[65] W. Ho, N. J. DiNiardo, and E. W. Plummer, J. Vac. Sci. Technol. **17**, 314 (1980).
[66] A. D. Johnson, K. J. Maynard, S. P. Daley, Q. Y. Yang, and S. T. Ceyer, Phys. Rev. Lett. **67**, 927 (1991).
[67] R. R. Cavanagh, R. D. Kelley, and J. J. Rush, J. Chem. Phys. **77**, 1540 (1982).
[68] M. Howard, U. A. Jayasooriya, S. F. A. Kettle, D. B. Powell, and N. Sheppard, J. Chem. Soc. Chem. Commun. **1**, 18 (1979).
[69] F. Muntean and P. B. Armentrout, J. Chem. Phys. **115**, 1213 (2001).
[70] M. E. Weber, J. L. Elkind, and P. B. Armentrout, J. Chem. Phys. **84**, 1521 (1986).
[71] J. L. Elkind and P. B. Armentrout, J. Phys. Chem. **90**, 6576 (1986).
[72] N. Aristov and P. B. Armentrout, J. Am. Chem. Soc. **108**, 1806 (1986).
[73] D. A. Hales and P. B. Armentrout, J. Cluster Sci. **1**, 127 (1990).
[74] H. Huber and G. Herzberg, *Constants of Diatomic Molecules* (Van Nostrand Reinhold, New York, 1979).
[75] P. B. Armentrout, in *Structure/Reactivity and Thermochemistry of Ions*, edited by P. Ausloos and S. G. Lias (D. Reidel, Dordrecht, 1987), p. 97.
[76] G. Gioumousis and D. P. Stevenson, J. Chem. Phys. **29**, 292 (1958).
[77] M. R. Zakin, D. M. Cox, R. O. Brickman, and A. Kaldor, J. Phys. Chem. **93**, 6823 (1989).
[78] G. Dietrich, K. Dagupta, S. Kuznestsov, K. Lützenkirchen, L. Schweikard, and J. Ziegler, Int. J. Mass Spectrom. Ion Processes **157**, 319 (1996).
[79] P. Siegbahn, M. Blomberg, I. Panas, and U. Wahlgren, Theor. Chim. Acta **75**, 143 (1989).
[80] P. B. Armentrout, in *Selective Hydrocarbon Activation: Principles and Progress*, edited by J. A. Davies, P. L. Watson, J. F. Liebman, and A. Greenberg (VCH, New York, 1990), p. 467.
[81] J. Sugar and C. Corliss, J. Phys. Chem. Ref. Data Suppl. **14**, 1 (1985).
[82] H. Basch, M. D. Newton, and J. W. Moskowitz, J. Chem. Phys. **73**, 4492 (1980).
[83] I. Shim and K. A. Gingerich, in *Physics and Chemistry of Small Clusters*, edited by P. Jena, B. K. Rao, and S. N. Khanna (Plenum, New York, 1987), p. 532.
[84] M. S. Daw and M. I. Baskes, Phys. Rev. B **29**, 6443 (1984).
[85] T. N. Truong, D. G. Truhlar, and B. C. Garrett, J. Phys. Chem. **93**, 8227 (1989).
[86] T. N. Truong and D. G. Truhlar, J. Phys. Chem. **94**, 8262 (1990).
[87] H. Yang and J. L. Whitten, J. Chem. Phys. **98**, 5039 (1992).
[88] J.-F. Paul and P. Sautet, Surf. Sci. **356**, L403 (1996).
[89] D. J. Klinke, II and L. J. Broadbelt, Surf. Sci. **429**, 169 (1999).
[90] K. Christmann, R. J. Behm, G. Ertl, M. A. Van Hove, and W. H. Weinberg, J. Chem. Phys. **70**, 4168 (1979).
[91] J. Lapujoulade and K. S. Neil, J. Chem. Phys. **57**, 34 (1972).

The Journal of Chemical Physics is copyrighted by the American Institute of Physics (AIP). Redistribution of journal material is subject to the AIP online journal license and/or AIP copyright. For more information, see http://ojps.aip.org/jcpo/jcpcr/jsp
Copyright of Journal of Chemical Physics is the property of American Institute of Physics and its content may not be copied or emailed to multiple sites or posted to a listserv without the copyright holder's express written permission. However, users may print, download, or email articles for individual use.